

Large positive magneto-conductivity at microwave frequencies in the compensated topological insulator BiSbTeSe₂

Mahasweta Bagchi,¹ Lea Pitz-Paal,¹ Christoph P. Grams,¹ Oliver Breunig,¹ Nick Borgwardt,¹ Zhiwei Wang,¹ Yoichi Ando,¹ Markus Grüninger,¹ and Joachim Hemberger^{1,*}

¹*Physics Institute II, University of Cologne, Zùlpicher Str. 77, D-50937 Cologne, Germany*

(Dated: February 12, 2019)

The bulk electronic properties of compensated topological insulators are strongly affected by the self-organized formation of charge puddles at low temperature, but their response in the microwave frequency range is little studied. We employed broadband impedance spectroscopy up to 5 GHz to address the ac transport properties of well-compensated BiSbTeSe₂, where charge puddles are known to form as metallic entities embedded in an insulating host. It turns out that the average puddle size sets the characteristic frequency ν_c in the GHz range, across which the insulating dc behavior is separated from a metal-like high-frequency response of delocalized carriers within the puddles. This ν_c is found to be controlled by a magnetic field, giving rise to a large positive magneto-conductivity observable only in the GHz range. This curious phenomenon is driven by the Zeeman energy which affects the local band filling in the disordered potential landscape to enhance the puddle size.

One of the most prominent features of topological insulators is the spin-momentum locking in the surface states [1], which is particularly useful for spintronic applications [2]. To efficiently utilize the spin-momentum-locked surface states in applications, one should get rid of the residual bulk conduction, and this has been achieved by carefully compensating residual donors by residual acceptors through composition tuning in the Bi_xSb_{2-x}Te_ySe_{3-y} compound [1, 3, 4]. Although such compensated topological insulators show reasonably high bulk insulation in dc, it has been elucidated that their transport properties are not only determined by the topologically protected surface states but also by the presence of charge puddles in the bulk [5], particularly at finite frequencies up to the infrared range [6]. This is because the Coulomb disorder of the randomly distributed charged donors and acceptors gives rise to potential fluctuations which grow as \sqrt{R} in a volume of size R^3 [5, 7]; this inevitably leads to the self-organized formation of charge puddles on a mesoscopic length scale L at low temperatures. On this length scale, portions of a sample contain delocalized charge carriers which give rise to a Drude-like contribution to the optical conductivity $\sigma'(\nu)$ above the Thouless cut-off frequency $2\pi\nu_c = D/L^2$ [6]. This cut-off is given by the time scale needed to diffuse through a puddle with the diffusion constant D . Using a simple scaling argument [5, 7], $L \approx 100 - 500$ nm is expected on the basis of infrared data [6]. This corresponds to ν_c in the GHz range.

Since the current-day information technology operates in the GHz range, understanding the microwave response of topological-insulator materials would be of crucial importance for their future applications in spintronics; nevertheless, the role of puddles in the transport properties in the GHz range has not yet been studied. This work is conceived to address this lack of understanding.

At low temperature, the Drude-like puddle contribution to $\sigma'(\nu)$ and its discrepancy with the dc conductivity have been observed in the well-compensated com-

pound BiSbTeSe₂ by Borgwardt *et al.* [6], who focused on infrared frequencies above the phonon range. Clear evidence for puddles stems in particular from the characteristic temperature-driven suppression of this Drude-like contribution on a temperature scale $k_B T = E_C$ set by the average Coulomb interaction E_C between neighboring dopants [6]. This “evaporation” of puddles is caused by thermally activated carriers which screen the Coulomb disorder. In BiSbTeSe₂, $E_C/k_B = 30 - 60$ K was observed [6, 8]. Also, puddles can explain the co-existence of electron-type and hole-type carriers in compensated samples [9] and the small activation energy observed in dc resistivity data [5]. Intriguingly, puddles are further found to be responsible for the surprising effect of gigantic negative magnetoresistance reported for TlBi_{0.15}Sb_{0.85}Te₂ [10]. In this context, novel magnetic-field effects would be expected in the vicinity of the cut-off frequency ν_c .

In this manuscript, we report on broadband spectroscopic investigations of BiSbTeSe₂ in the cut-off frequency range to look for the ac conductivity behavior associated with charge puddles and their response to magnetic fields. Our central result is the discovery of a large positive magneto-conductivity at microwave frequencies, which arises due to the change of the puddle size by an external magnetic field. In addition, our data provide solid understanding of the role of puddles in the transport properties in the GHz range, providing foundations for future high-frequency applications of topological insulators.

Single crystals of BiSbTeSe₂ were grown from a melt of high-purity starting elements Bi, Sb, Te, and Se by using a modified Bridgman method in a sealed quartz-glass tube as described elsewhere [4]. For the microwave measurements, we used scotch-tape-cleaved flakes with length $l \approx 1$ mm, width $w \approx 1$ mm, and thickness $t \approx 20$ μ m; the possible error in the determination of t leads to an uncertainty in the absolute values of about 10%.

The measurements were performed in a commercial ^4He -flow cryo-magnet (QUANTUM-DESIGN PPMS) employing four point geometry for the dc measurements and a home-made, two point coaxial-line inset for the microwave range. The complex frequency-dependent conductivity $\sigma(\nu) = \sigma'(\nu) + i\sigma''(\nu)$ was measured using a coplanar waveguide setup for frequencies up to 5 GHz evaluating the complex scattering coefficients S_{12} and S_{22} gained via a vector network analyzer (ZNB8, ROHDE&SCHWARZ). All measurements were performed with the electric field perpendicular to the crystallographic c axis. The contacts were applied using silver paint. The lower boundary of the microwave measurement range is set by the influence of the contact electrodes. At the contact interfaces, the formation of Schottky-type depletion layers can lead to Maxwell-Wagner type effects [11] giving an additional capacitive contribution C_C and a serial contact resistance R_C . Together, they form a RC element in series with the intrinsic sample impedance. The contacts thus are short-cut for frequencies $2\pi\nu > 1/R_C C_C$ [12, 13]. This allows us to reliably evaluate the intrinsic sample conductivity for frequencies above 30 MHz, as illustrated in Fig. S1 of the Supplemental Material [14].

The length scale L of puddle formation is connected to a time scale $1/\nu_c = 2\pi L^2/D$ on which the locally uncompensated carriers behave like free charges. For larger times or lengths, carrier motion is hindered by the puddle boundaries. This leads to insulating behavior for dc or low-frequency transport measurements and to a Drude-like metallic conductivity at high frequencies which is cut off below ν_c . Assuming that puddles form as soon as the fluctuations of the Coulomb potential are as large as $\Delta/2$, where Δ denotes the band gap, Shklovskii and coworkers [5, 7] estimated L via a simple scaling argument,

$$L = \frac{(\Delta/E_C)^2}{8\pi N_{\text{def}}^{1/3}}, \quad (1)$$

where N_{def} is the defect density of acceptors and donors, and the average Coulomb interaction between neighboring dopants is given by $E_C = N_{\text{def}}^{1/3} e^2 / (4\pi\epsilon_0\epsilon)$ with the permittivity ϵ . For BiSbTeSe₂, infrared data show $\Delta = 0.26$ eV and $\epsilon \approx 200$ [6]. Note that N_{def} and thus also E_C are sample-dependent quantities. For two different samples of BiSbTeSe₂, $E_C/k_B = 30$ –40 K and 40–60 K were reported, resulting in $N_{\text{def}} = 0.5$ – $1.1 \cdot 10^{20}$ cm⁻³ and 1 – $4 \cdot 10^{20}$ cm⁻³, respectively [6, 8]. This is equivalent to $\Delta/E_C \approx 50$ –100 and $L \approx 140$ –1000 nm. Using a diffusion constant of $D \approx 2$ cm²/s [6], we find $\nu_c \lesssim 2$ GHz. Note, however, that direct experimental values for L or ν_c are still lacking.

Bömerich *et al.* [15] used a numerical approach combined with a refined scaling argument and found smaller values for the length scale L . An experimental lower limit is provided by the length scale $r_s = 40$ –50 nm observed

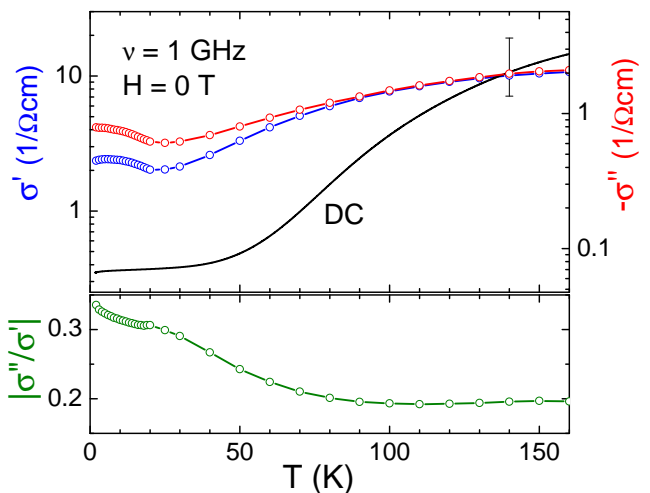


FIG. 1: Top: dc and ac (1 GHz) conductivity σ' in compensated BiSbTeSe₂. The error bar denotes the uncertainty in the absolute values. These vary by about a factor of 3 for samples with the same nominal composition, which partially can be attributed to different defect densities [4]. Bottom: The ratio $|\sigma''/\sigma'|$ is constant at high temperature, in agreement with variable range hopping. For puddle formation, an increase of $|\sigma''/\sigma'|$ at low temperature is expected for frequencies close to ν_c .

for *surface* puddles by scanning tunnelling microscopy in BiSbTeSe₂ [8]. The Dirac carriers on the surface give rise to enhanced screening, one thus expects $r_s < L$. Experimentally, the defect density may not only be sample dependent but it may also vary within a given sample. Thus, one has to expect a distribution of puddle sizes and concomitantly a distribution of cut-off frequencies, giving rise to a considerably broadened features in the dynamic response. For BiSbTeSe₂, the above discussed limits of L , 40 nm and 1000 nm, span a broad frequency range of 0.03 to 20 GHz for the distribution of ν_c .

Clear fingerprints of puddle formation are found in the temperature dependence of the conductivity (Fig. 1). We observe the expected discrepancy between dc and ac conductivities at low temperature, while the high-temperature data agree within the experimental error bar. At the lowest measured temperatures, the dc conductivity lies more than one decade below the ac data measured at 1 GHz. The contribution of puddles is most evident from the reincrease of the ac conductivity below roughly 30 K, which agrees with the energy scale E_C found in the infrared data [6]. Note that variable range hopping (VRH) also gives rise to an enhanced ac conductivity, which explains the behavior at higher temperatures. In BiSbTeSe₂, VRH has been shown to describe the dc resistivity in a temperature window above about 80 K [4]. In the ac conductivity, VRH gives rise to a contribution to both $\sigma'(\nu)$ and $\sigma''(\nu)$ that scales with a power law ν^s with $s < 1$ [16]. This scaling behavior results in a fixed ratio $|\sigma''/\sigma'|$ over a wide range in tem-

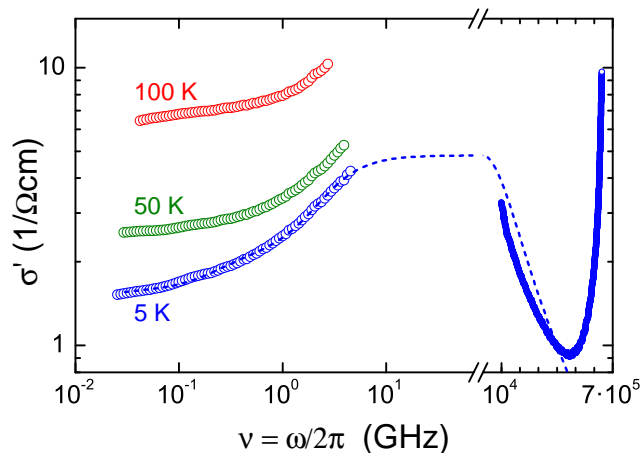


FIG. 2: Left part: Broadband microwave conductivity spectra of BiSbTeSe₂ on a logarithmic frequency scale for selected temperatures. Right part (beyond axis break): Infrared data of a different sample of BiSbTeSe₂ [6] on a linear frequency scale. The strong onset of $\sigma'(\nu)$ above about 63 THz or 0.26 eV corresponds to the band gap. Dashed line: fit to the Drude-like contribution of puddles assuming a distribution of cut-off frequencies as described in the text. The difference in Drude weight between different samples of BiSbTeSe₂ can at least partially be attributed to a sample dependence of the defect density, reflecting itself in a variation of the dc resistivity by a factor of about 3.

perature and frequency [17, 18]. In BiSbTeSe₂, we find such a constant ratio at 1 GHz above about 70 K, see bottom panel of Fig. 1. In contrast, the increase of $|\sigma''/\sigma'|$ at lower temperatures can be attributed to the formation of polarizable puddles with a finite cut-off frequency ν_c resulting in a considerable contribution to σ'' . This additional increase of σ'' is also evident in the top panel of Fig. 1.

Figure 2 shows broadband microwave spectra of the conductivity $\sigma'(\nu)$ for different temperatures. We observe an increase of $\sigma'(\nu)$ with increasing ν below 5 GHz. Importantly, this increase is more pronounced at 5 K than at 50 K or 100 K, i.e., the frequency dependence is larger at a temperature where puddles have formed. The overall much larger value of $\sigma'(\nu)$ at higher temperatures and its weaker frequency dependence correspond to the metallic Drude contribution of *thermally activated* carriers, as also observed in the infrared range [6]. The low-temperature behavior can be attributed to a smeared-out cut-off of the Drude-like contribution of puddles at frequencies of the order of 1 GHz. To quantitatively analyse this behavior, we fitted the 5 K data by considering Drude-Lorentz oscillators, see dashed line in Fig. 2: In this fitting, the damping $\Gamma = 21$ THz was fixed to the value determined from the infrared data [6]; to take into account the distribution of the puddle size in which the charge carriers are confined, we approximated the situation as a sum of three broad Lorentzians centered at

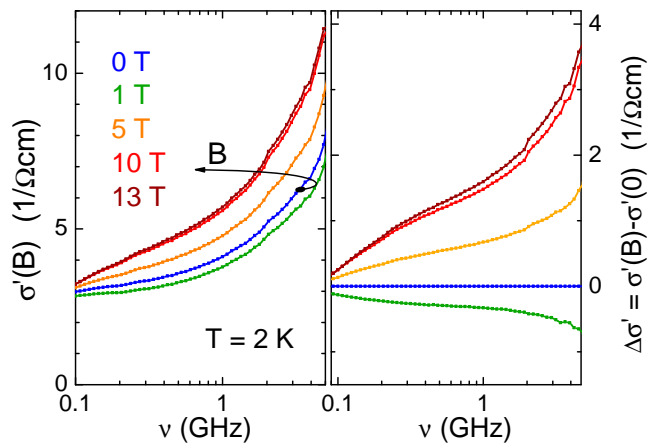


FIG. 3: Left: Conductivity spectra measured at $T = 2$ K for various values of the external magnetic field up to 13 T. Right: Magnetic field dependent contribution to the conductivity spectra as gained by subtraction of the zero field data.

9.3 GHz, 72 GHz, and 234 GHz (these frequencies are optimized to best reproduce the data). For such overdamped oscillators, this distribution gives an effective cut-off frequency $\nu_c \approx \nu_0^2/\Gamma \lesssim 3$ GHz. Also, this distribution of the eigenfrequencies corresponds to a range of the puddle size L of 0.1 – 3 μm , when we use D given in Ref. [6]. One can see in Fig. 2 that this model reproduces both the low and high frequency behavior of $\sigma'(\nu)$ reasonably well, giving confidence that the overall behavior of $\sigma'(\nu)$ is governed by puddles.

An external magnetic field influences the size of puddles, as shown recently by Breunig *et al.* [10] in the nearly bulk-insulating topological insulator TlBi_{0.15}Sb_{0.85}Te₂ by dc resistivity measurements. Puddles form when the bands touch the chemical potential due to the spatial fluctuations of the Coulomb potential. The magnetic field does not change the Coulomb potential but the Zeeman energy shifts the band bottom/top with respect to the disordered potential landscape and thereby affects the puddle size [10]. The compound TlBi_{0.15}Sb_{0.85}Te₂ studied in Ref. [10] is less well compensated than BiSbTeSe₂ and the low-temperature conductivity is determined by percolating current paths formed in the disordered bulk. A field-induced change of the puddle size leads to a strong increase of percolating puddles and hence a gigantic field-induced reduction of the dc resistance [10]. In contrast, BiSbTeSe₂ is well compensated. Puddles do not percolate, the bulk resistivity at low temperatures is much higher, and the influence of a magnetic field on the dc conductivity is expected to be much weaker as long as the percolation limit is not reached. Close to the cut-off frequency, however, a magnetic-field-induced change of the puddle size may have considerable impact.

Figure 3 shows $\sigma'(\nu)$ at 2 K for different values of the

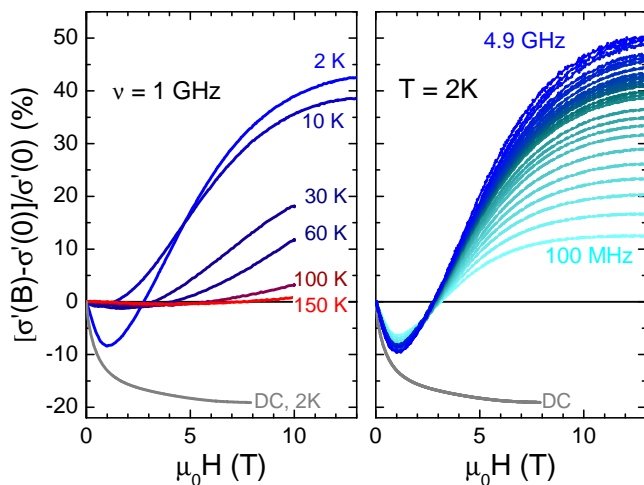


FIG. 4: Left: Normalized magneto-conductivity measured at 1 GHz for various temperatures from 2 K to 150 K. Right: Normalized magneto-conductivity measured at $T = 2$ K for different frequencies in equidistant logarithmic spacing between 100 MHz and 4.9 GHz. The dc conductivity at 2 K (gray) is displayed for comparison.

external magnetic field. One can see that the behavior at 1 T is clearly different from that at higher fields; namely, the conductivity in 1 T is lower than in zero field and the difference increases with increasing frequency, as is evident in the right panel. At such low fields, the ac transport is dominated by weak anti-localization (WAL) characteristic for disordered systems with strong spin-orbit coupling [1, 20, 21]. The suppression of WAL in small magnetic fields leads to localization of carriers and therefore to a reduced conductivity. In contrast, in higher fields the conductivity increases strongly, in particular at higher frequencies. This can be attributed to a field-induced shift of the cut-off frequency ν_c that is triggered by a field-induced change of the puddle size. This shift is directly visualized in the left panel of Fig. 3 via the shift of the rise in $\sigma'(\nu)$.

At high fields, the suppression of weak anti-localization still applies but it is overruled by the strong positive ac magneto-conductivity. This is evident in the left panel of Fig. 4, which depicts the normalized magneto-conductivity $[\sigma'(B) - \sigma'(0)]/\sigma'(0)$ at 1 GHz as a function of the external magnetic field. The “dip” below 3 T is due to the WAL effect discussed above, but a pronounced positive magneto-conductivity sets in at higher fields. As shown in the right panel of Fig. 4, the high-field magneto-conductivity strongly increases with frequency, reaching 50% in 13 T at 4.9 GHz. The dc data shown in Fig. 4 for comparison is governed by the WAL all the way up to high fields and only presents negative magneto-conductivity approaching -20% at high magnetic field. This crossover in the high-field magneto-conductance from negative to positive upon changing

from dc to the microwave range shows that it is not a field-induced percolation which dominates transport properties in compensated BiSbTeSe_2 . Rather, the magnetic field mainly affects the average size of still isolated puddles. The corresponding shift of the cut-off frequency ν_c naturally explains the large magneto-conductivity at frequencies in the vicinity of ν_c in the GHz range.

In the left panel of Fig. 4, one can also see how the magneto-conductivity behavior at 1 GHz changes with temperature. The pronounced positive microwave magneto-conductivity is limited to the low-temperature range where charge puddles are present. At higher temperatures ($\gtrsim 30$ K) where puddles have evaporated, the magneto-conductivity is drastically suppressed.

In conclusion, we have demonstrated that the ac transport properties of the compensated topological insulator BiSbTeSe_2 at low temperatures are determined by the presence of charge puddles, which gives rise to an unusual positive magneto-conductivity observable only in the GHz range. The random nature of the Coulomb-potential fluctuations causes a distribution of the puddle size, which leads to a broad cut-off regime in the microwave range separating the insulating dc behavior from the metal-like ac response; our analysis shows that the overall ac conductivity behavior points to the puddle-size distribution of $0.1 - 3 \mu\text{m}$. The remarkable effect of the magnetic field to enlarge the puddle size, previously suggested in Ref. [10] for an imperfectly compensated topological insulator, is now found to cause a large positive magneto-conductivity even in a well-compensated system near the characteristic cut-off frequency. Hence, tailoring the defect density and the corresponding disorder-induced microstructure will be of crucial importance to any potential applications of bulk topological insulators in the technologically important GHz range.

Acknowledgements

The authors thank A. Rosch for valuable discussions. This work was funded by the Deutsche Forschungsgemeinschaft (DFG, German Research Foundation) – Project number 277146847 – CRC 1238 (projects A04 and B02).

* Corresponding author: hemberger@ph2.uni-koeln.de

- [1] Y. Ando, *Topological insulator materials*, J. Phys. Soc. Jpn **82**, 102001 (2013)
- [2] D. Pesin and A. H. MacDonald, *Spintronics and pseudospintronics in graphene and topological insulators*, Nat. Mater. **11**, 409 (2012).
- [3] A.A. Taskin, Z. Ren, S. Sasaki, K. Segawa, and Y. Ando, *Observation of Dirac Holes and Electrons in a Topological Insulator*, Phys. Rev. Lett. **107**, 016801 (2011).
- [4] Z. Ren, A.A. Taskin, S. Sasaki, K. Segawa, and Y. Ando, *Optimizing $\text{Bi}_{2-x}\text{Sb}_x\text{Te}_{3-y}\text{Se}_y$ solid solutions to approach the intrinsic topological insulator regime*, Phys. Rev. B **84**, 165311 (2011).

- [5] B. Skinner, T. Chen, and B.I. Shklovskii, *Why Is the Bulk Resistivity of Topological Insulators So Small?*, Phys. Rev. Lett. **109**, 176801 (2012).
- [6] N. Borgwardt, J. Lux, I. Vergara, Z. Wang, A.A. Taskin, K. Segawa, P.H.M. van Loosdrecht, Y. Ando, A. Rosch, and M. Grüninger, *Self-organized charge puddles in a three-dimensional topological material*, Phys. Rev. B **93**, 245149 (2016).
- [7] B. I. Shklovskii and A. L. Efros, *Completely Compensated Crystalline Semiconductor as a Model of an Amorphous Semiconductor*, Sov. Phys. JETP **35**, 610 (1972).
- [8] T. Knispel, W. Jolie, N. Borgwardt, J. Lux, Zhiwei Wang, Yoichi Ando, A. Rosch, T. Michely, and M. Grüninger, *Charge puddles in the bulk and on the surface of the topological insulator BiSbTeSe₂ studied by scanning tunneling microscopy and optical spectroscopy*, Phys. Rev. B **96**, 195135 (2017).
- [9] C.W. Rischau, A. Ubaldini, E. Giannini, and C.J. van der Beek, *Charge puddles in a completely compensated topological insulator*, New J. Phys. **18**, 073024 (2016).
- [10] O. Breunig, Z. Wang, A.A. Taskin, J. Lux, A. Rosch, and Y. Ando, *Gigantic negative magnetoresistance in the bulk of a disordered topological insulator*, Nat. Comm. **8**, 15545 (2017).
- [11] J.C. Maxwell, *Treatise on Electricity and Magnetism*, 3rd ed. (Dover, New York, 1991).
- [12] P. Lunkenheimer, V. Bobnar, A. V. Pronin, A. I. Ritus, A. A. Volkov, and A. Loidl *Origin of apparent colossal dielectric constants*, Phys. Rev. B **66**, 052105 (2002).
- [13] D. Niermann, F. Waschkowski, J. de Groot, M. Angst, and J. Hemberger, *Dielectric Properties of Charge-Ordered LuFe₂O₄ Revisited: The Apparent Influence of Contacts*, Phys. Rev. Lett. **109**, 016405 (2012).
- [14] See Supplemental Material at [URL] for supplemental data and discussions.
- [15] T. Bömerich, J. Lux, Q.T. Feng, and A. Rosch, *Length scale of puddle formation in compensation-doped semiconductors and topological insulators*, Phys. Rev. B **96**, 075204 (2017).
- [16] P. Lunkenheimer and A. Loidl, *Response of Disordered Matter to Electromagnetic Fields*, Phys. Rev. Lett. **91**, 207601 (2003).
- [17] A.K. Jonscher, *Universal Relaxation Law* (Chelsea, New York, 1996).
- [18] S.R. Elliott, *A.c. conduction in amorphous chalcogenide and pnictide semiconductors*, Adv. Phys. **36**, 135 (1987).
- [19] A. Segura, V. Panchal, J. F. Sánchez-Royo, V. Marín-Borrás, V. Muñoz-Sanjosé, P. Rodríguez-Hernández, A. Muñoz, E. Pérez-González, F. J. Manjón, and J. González, *Trapping of three-dimensional electrons and transition to two-dimensional transport in the three-dimensional topological insulator Bi₂Se₃ under high pressure*, Phys. Rev. B **85**, 195139 (2012).
- [20] B. Altshuler, A.G. Aronov, A.I. Larkin, and D.E. Khmel'nitskil, *Anomalous magnetoresistance in semiconductors*, Sov. Phys. JETP **54**, 411 (1981).
- [21] S. Hikami, A. I. Larkin, and Y. Nagaoka, *Spin-Orbit Interaction and Magnetoresistance in the Two Dimensional Random System*, Prog. Theor. Phys. **63**, 707 (1980).

Supplemental Material

Effect of Electrical Contacts

Schottky-type depletion layers tend to form at the electrical contact formed at interfaces between sample and silver electrodes. The depletion layers lead to Maxwell-Wagner type contributions to the complex impedance $Z^*(\omega)$ [11]. These can be modelled employing an equivalent circuit containing an additional capacitive contribution C_C and a contact resistance R_C . Together, they form an RC element in series with the intrinsic sample impedance. The resulting impedance thus can be described as

$$Z^* = \frac{R_c}{1 + \omega^2 \tau_c^2} + \frac{R_s}{1 + \omega^2 \tau_s^2} - i \left(\frac{R_C \omega \tau_c}{1 + \omega^2 \tau_c^2} + \frac{R_s \omega \tau_s}{1 + \omega^2 \tau_s^2} \right)$$

with the relaxation times $\tau_c = R_c C_c$ and $\tau_s = R_s C_s$ for contacts and sample, respectively. Usually, the thin contact depletion layers lead to $\tau_c \gg \tau_s$ and the contacts thus are short-cut for frequencies $2\pi\nu > 1/\tau_c$ [12, 13]. In addition one can expand the accessible frequency range by subtracting the contact contribution, which dominates the low frequency range and therefore can be fitted for $2\pi\nu < 1/\tau_c$. The remaining impedance can be evaluated via the geometry factor A/d with respect to the complex conductivity $\sigma' = A/d \cdot Z'/Z^2$ and $\sigma'' = A/d \cdot Z''/Z^2$.

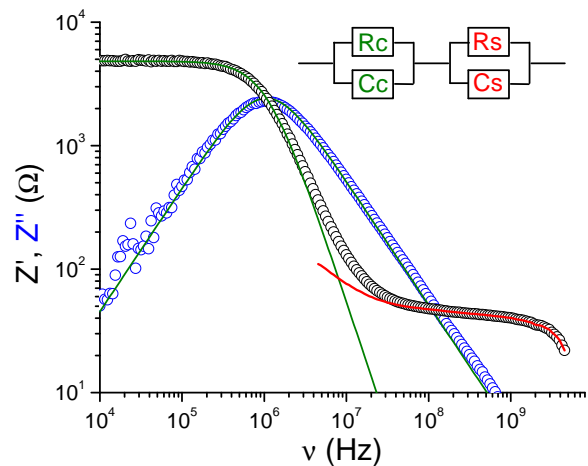


FIG. S1: Frequency dependence of the measured complex impedance Z^* at 300 K (circles), which is dominated by the contacts at low frequencies and by the sample impedance at high frequencies. The contribution of the contacts is depicted by the solid green line, assuming an RC element with constant values for R_C and C_C . The solid red line represents the intrinsic sample contribution given by $R_s(\nu)$ and $C_s(\nu)$. The sketch in the inset shows the corresponding equivalent circuit.